Energy & Environmental Science

COMMUNICATION

View Article Online
View Journal

Cite this: DOI: 10.1039/c8ee02924e

Received 4th October 2018,
Accepted 16th November 2018

DOI: 10.1039/c8ee02924e

rsc.li/ees

Ultrahigh-voltage integrated micro-supercapacitors with designable shapes and superior flexibility†‡

Xiaoyu Shi,§[abc] Songfeng Pei,§[d] Feng Zhou,[a] Wencai Ren,*[d] Hui-Ming Cheng,[de] Zhong-Shuai Wu*[a] and Xinhe Bao[ab]

With the development of power source-integrated electronics, the miniaturization of high-voltage integrated micro-supercapacitors (IMSCs) with multiple innovative form factors is urgently required but remains unsolved. Here, we demonstrate a universal, cost-effective, industrially applicable protocol for fast and scalable fabrication of graphene-based planar IMSCs, with shape diversity, aesthetic versatility, outstanding flexibility and superior modularization. Using highly-conducting graphene ink, we directly screen-print shape-designable IMSCs in several seconds, consisting of hundreds to thousands of individual MSCs on arbitrary substrates. The resulting IMSCs are free of external metal current collectors and interconnects as well as separators, and exhibit exceptional electrical double-layer capacitive behaviors and remarkable flexibility. Notably, the output voltage and capacitance of IMSCs are readily adjustable through connection in well-defined arrangements of MSCs. As a proof of concept, a tandem energy storage pack of IMSCs with 130 MSCs can output a recorded voltage exceeding 100 V, demonstrative of superior modularization and performance uniformity.

Broader context

The unprecedented boom of microelectronics has stimulated the urgent demand for microscale energy storage devices with multiple innovative form factors, *e.g.*, flexibility, shape diversity, high voltage, and tailored capacitance, serving as microscale power sources for seamless integration with miniature electronics. Planar micro-supercapacitors (MSCs), consisting of two adjacent electrodes separated by a separator-free interspace on a single substrate, could substantially simplify the integration process and avoid the possibility of multilayer delamination under bending states, thereby holding great potential for actual applications. However, cost-effective, scalable fabrication of integrated MSCs (IMSCs) with high voltage output is still unsolved. To this end, a low-cost, industrially applicable screen-printing protocol was developed for creating ultrahigh-voltage IMSCs, with designable shapes, aesthetic versatility, outstanding flexibility and superior modularization. Shape-designable IMSCs, free of external metal current collectors and interconnects, can be readily produced in several seconds, consisting of hundreds to thousands of individual MSCs. As a proof of concept, IMSCs with serially-connected 130 single cells can output a recorded voltage of more than 100 V, indicative of superior modularization and performance uniformity. This work will pave the way for scalable fabrication of microscale planar energy storage devices, with high voltage output, for various power source-integrated microelectronics.

Introduction

High-voltage microscale energy storage devices with an adjustable output of tens to thousands of volts are urgently required for high-voltage applications of miniature electronics and micromachines, like microrobots, soft actuators, skin electronics, health monitors, and microsensors.[1–6] Conventional microscale supercapacitors and batteries with a nonplanar stacked geometry not only suffer from bulky volume, heavy weight, limited flexibility, and fixed shape, but also represent huge inconvenient device connection in series using lots of conducting metal wires to offer high-voltage output; therefore, both of them cannot satisfy the stringent requirements of high-voltage electronic devices.[7] Recently, micro-supercapacitors (MSCs) with a planar geometry are intensively exploited as a competitive class of on-chip power sources.[8] More significantly, such planar MSCs built on a single substrate are highly favourable for engineering integrated MSCs (IMSCs),[9,10] free of traditional metal interconnects and separators, which can potentially boost high-voltage output,

[a] Dalian National Laboratory for Clean Energy, Dalian Institute of Chemical Physics, Chinese Academy of Sciences, 457 Zhongshan Road, Dalian 116023, China. E-mail: wuzs@dicp.ac.cn
[b] State Key Laboratory of Catalysis, Dalian Institute of Chemical Physics, Chinese Academy of Sciences, 457 Zhongshan Road, Dalian 116023, China
[c] Department of Chemical Physics, University of Science and Technology of China, 96 JinZhai Road, Hefei 230026, P. R. China
[d] Shenyang National Laboratory for Materials Science, Institute of Metal Research, Chinese Academy of Sciences, 72 Wenhua Road, Shenyang 110016, P. R. China. E-mail: wcren@imr.ac.cn
[e] Tsinghua-Berkeley Shenzhen Institute, 1001 Xueyuan Road, Shenzhen 518055, China

† Dedicated to the 70th anniversary of Dalian Institute of Chemical Physics, CAS.
‡ Electronic supplementary information (ESI) available. See DOI: 10.1039/c8ee02924e
§ These authors contributed equally.

and simultaneously combine multiple smart characteristics of designable shapes, tailored sizes, lightweight, space-saving connections, and superior flexibility.

So far, great advancements have been made for MSCs,[11–18] through the development of nanostructural electrode materials of pseudocapacitive metal oxides/hydroxides,[14,19–22] conducting polymers,[23,24] and capacitive nanocarbons.[8,25] More recently, graphene[26,27] and two-dimensional (2D) materials[28] (e.g., MXenes,[29,30] phosphorene,[31] thiophene,[32] and MnO_2[33]) have been emerging as a promising class of electrode materials for MSCs because they present large surface area, ultra-thinness, and robust flexibility, allowing for ultrafast shuttling of electrolyte ions along the plane of 2D nanosheets.[34] Meanwhile, diverse microfabrication technologies, e.g., photolithography,[35] laser-scribing,[36,37] photochemical reduction,[38] mask-assisted patterning,[31] and scalable printing,[39,40] have been demonstrated for planar MSCs.

Despite the enormous progress of MSCs, scalable production of high-voltage IMSCs is still challenging. First, popular photolithographic techniques involving expensive equipment and complicated steps significantly increase the cost and prevent the fast production of IMSCs on a large scale. Second, metal current collectors and interconnects are required for the integration of MSCs, resulting in reduced gravimetric and volumetric capacitances, and unsatisfactory flexibility of IMSCs. Third, printing techniques, *e.g.*, spray coating,[41,42] inkjet printing,[39,40] screen printing,[43,44] and 3D printing,[45–47] are simple and cost-effective, but printable MSCs usually show poor modularization with limited voltage (normally <10 V), and are short of ink with high conductivity, capacitance and suitable rheological properties, acting as both active materials and interconnects of IMSCs, while exploiting advantages of high resolution, efficiency and integration of printing. Therefore, fast and scalable fabrication of high-voltage IMSCs has not yet been achieved.

Here we report the first demonstration of ultrahigh-voltage IMSCs (denoted SPG-IMSCs) based on in-series screen-printed graphene (SPG) on various substrates, with a highly stable and conductive ink. The whole printing process could be finished in several seconds, and without the requirements of expensive equipment and harsh conditions, indicative of the high efficiency, cost-effectiveness and scalability of our technique. In addition, the resulting IMSCs exhibited tailored capacitance, exceptional flexibility, shape diversity, aesthetic versatility, superior integration, and without the need for metal current collectors and wires, manifesting great potential as power sources of future printed electronics.

Results and discussion

Preparation of ink and fabrication of IMSCs

The screen printing fabrication of SPG-IMSCs is schematically illustrated in Fig. 1a. First, a highly stable and conductive ink

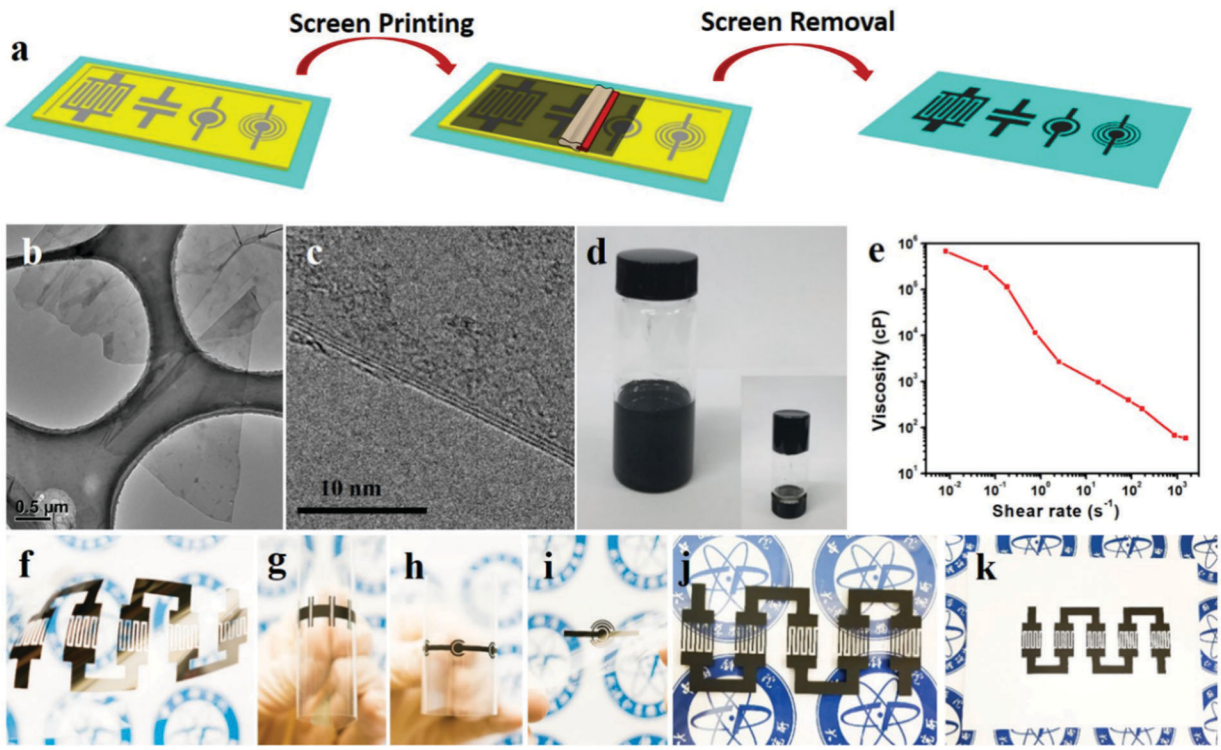

Fig. 1 Fabrication and characterization of SPG-IMSCs. (a) Schematic of the fabrication process of SPG-IMSCs with diverse planar geometries. (b) Transmission electron microscopy (TEM) and (c) high-resolution TEM images of graphene. (d) Photographs of graphene-based ink. (e) Viscosity of graphene-based ink as a function of shear rate. Photographs of SPG-IMSCs with diverse geometries, *e.g.*, (f) interdigital, (g) parallel strip, (h) concentric circle and (i) circular interdigital shapes on PET substrates. Photographs of tandem SPG-IMSCs with an interdigital geometry on (j) glass and (k) A4 paper.

(Fig. 1d) was prepared by mixing high-quality graphene with a large lateral size of 5–10 μm and a high C/O ratio of >17 (Fig. 1b and c and Fig. S1–S5, ESI‡), conducting carbon black and poly(vinyl chloride-*co*-vinyl acetate) (P-VC/VAc) binder in dimethyl mixed dibasic acid ester (DBE) solvent. The resulting ink exhibits outstanding shear-thinning behaviour, allowing for extrusion of the ink through screen meshes under shear force and its quick solidification without shear force,[12,48] extremely suitable for screen printing (Fig. 1e). Second, an insulative substrate (*e.g.*, polyethylene terephthalate (PET), A4 paper, glass, or cloth) was placed below the customized screen with patterned meshes, and thus the ink was extruded through the screen for deposition on the placed substrate. After screen removal and drying of the patterned microelectrodes, a gel electrolyte of polyvinyl alcohol/H_3PO_4 (PVA/H_3PO_4) was carefully dropped onto the projected area of microelectrodes and solidified. Finally, all-solid-state SPG-IMSCs were obtained. It is noted that, different from the photolithographic technique, this strategy is highly scalable for fast and low-cost production of SPG-IMSCs with outstanding flexibility, diverse sizes, and complex planar geometries, *e.g.*, interdigital finger, strip, concentric circle, and circular interdigital patterns (Fig. 1f–i) on various substrates (Fig. 1j and k), and SPG films exhibited large-area uniformity (Fig. S6, ESI‡). Moreover, large-scale modularization of SPG-IMSCs with the designable patterns of microelectrodes, current collectors, and interconnects, *via* in parallel and in series, and in arbitrary arrangements to tailor the performance, can be readily manufactured within seconds by one-step screen printing of graphene ink, without external metal current collectors and interconnects, demonstrative of an industrially applicable protocol for the production of IMSCs.

Electrochemical characterization of single MSC

To demonstrate the remarkable performance of SPG-IMSCs, we first carried out electrochemical characterization of individual MSCs based on SPG interdigital patterns (denoted SPG-MSCs) in PVA/H_3PO_4 electrolyte on PET substrates (Fig. 2a and b), using cyclic voltammetry (CV) curves at scan rates from 5 to 500 mV s^{-1} (Fig. 2c and d), galvanostatic charge–discharge (GCD) profiles at current densities of 0.01 to 0.1 mA cm^{-2} (Fig. 2f), and electrochemical impedance spectroscopy data (EIS, Fig. S7, ESI‡). Notably, SPG-MSCs exhibited approximately rectangular CV

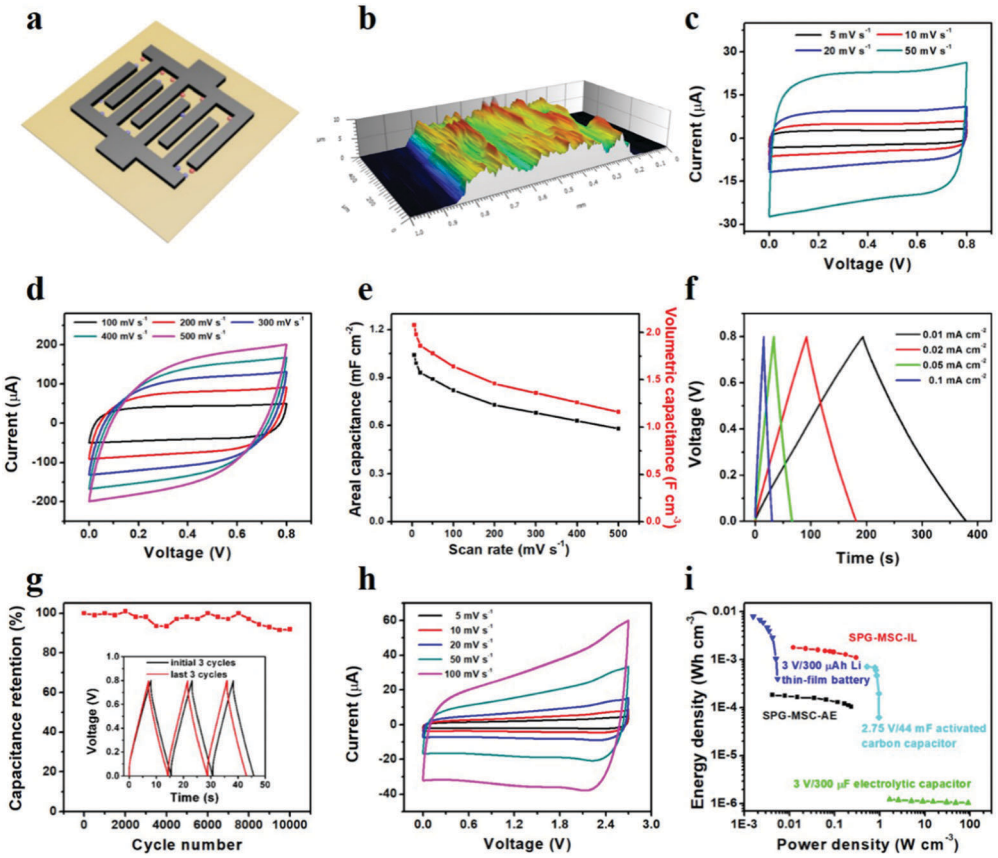

Fig. 2 Electrochemical characterization of interdigital SPG-MSCs on a PET substrate. (a) Schematic of an interdigital SPG-MSC. (b) 3D profile of a finger electrode of SPG-MSCs on PET, showing an average thickness of about 5 μm. CV curves of SPG-MSCs obtained at different scan rates (c) from 5 to 50 mV s^{-1} and (d) from 100 to 500 mV s^{-1} in PVA/H_3PO_4 electrolyte. The SPG-MSCs tested in PVA/H_3PO_4 are denoted as SPG-MSCs-AE. (e) Areal capacitance and volumetric capacitance of SPG-MSCs-AE as functions of scan rate. (f) GCD profiles of SPG-MSCs-AE tested at current densities from 0.01 to 0.1 mA cm^{-2}. (g) Cycling stability of SPG-MSCs-AE for 10 000 cycles at a current density of 0.2 mA cm^{-2}. Inset: Three GCD curves of SPG-MSCs-AE before and after cycling. (h) CV curves of SPG-MSCs obtained at different scan rates from 5 to 100 mV s^{-1} in $EMIMNTF_2$. The SPG-MSCs tested in ionic liquid are denoted as SPG-MSCs-IL. (i) Ragone plots of SPG-MSCs in gel and ionic liquid electrolytes.

curves even at a high scan rate of 500 mV s^{-1}, indicative of robust electrical double-layer capacitive (EDLC) behaviour. This result was also validated by GCD profiles, representing nearly symmetrical triangle shapes (Fig. 2f). Further, the areal capacitance of SPG-MSCs was calculated to be 1.0 mF cm^{-2} at 5 mV s^{-1} (Fig. 2e), well comparable to those of most reported graphene MSCs, such as methane plasma reduced graphene oxide (rGO, 0.08 mF cm^{-2}),[49] inkjet-printed graphene (0.7 mF cm^{-2}),[40] laser written graphene (0.51 mF cm^{-2}),[50] and photochemically reduced GO (1.5 mF cm^{-2}).[38] Also, SPG-MSCs showed superior rate performance, with a significant capacitance of 0.58 mF cm^{-2} maintained even at a high scan rate of 500 mV s^{-1}, resulting from the high electrical conductivity of the SPG microelectrodes (~36 S cm^{-1}). Meanwhile, 91.8% of the capacitance was retained after 10 000 cycles (Fig. 2g). Our SPG-MSCs also displayed an impressive areal capacitance of 0.89 mF cm^{-2}, a high energy density of 1.81 mW h cm^{-3} and a power density of 297 mW cm^{-3} in an ionic liquid electrolyte of 1-ethyl-3-methylimidazolium bis(trifluoromethylsulfonyl)imide ($EMIMNTF_2$) (Fig. 2h and i and Fig. S8, ESI‡), and exhibited ideal EDLC behaviours on other insulative substrates, *e.g.*, glass and A4 paper (Fig. S9 and S10, ESI‡), implying wide applicability of our technique.

Shape diversity and flexibility

To further highlight the shape diversity and performance uniformity of our devices, we constructed several shape-designable tandem SPG-IMSCs, with concentric circle, linear and foldable planar geometries, and their microelectrode size parameters are shown in Fig. S11 (ESI‡), *via* serial connection of 3 or 4 cells on PET (Fig. 3a–c), A4 paper and glass (Fig. S19, ESI‡) substrates. Remarkably, all these versatile-shaped SPG-IMSCs exhibited similar CV curves and approximately equal areal capacitances at a low scan rate of 5 mV s^{-1} (Fig. 3d and e), demonstrative of exceptionally good shape conformability and wide applicability. It is noted that the foldable SPG-MSCs showed low rate capability, with an initial capacitance of 21% at 100 mV s^{-1}, inferior to those of the other three geometries (62–79%), implying that the narrower electrodes and interspaces, and the shorter lengths of microelectrodes would significantly contribute to higher rate capability (Fig. 3f and Fig. S12–S14, ESI‡).[9,35,51] Furthermore, these SPG-IMSCs exhibited ideal tandem capacitive behaviours

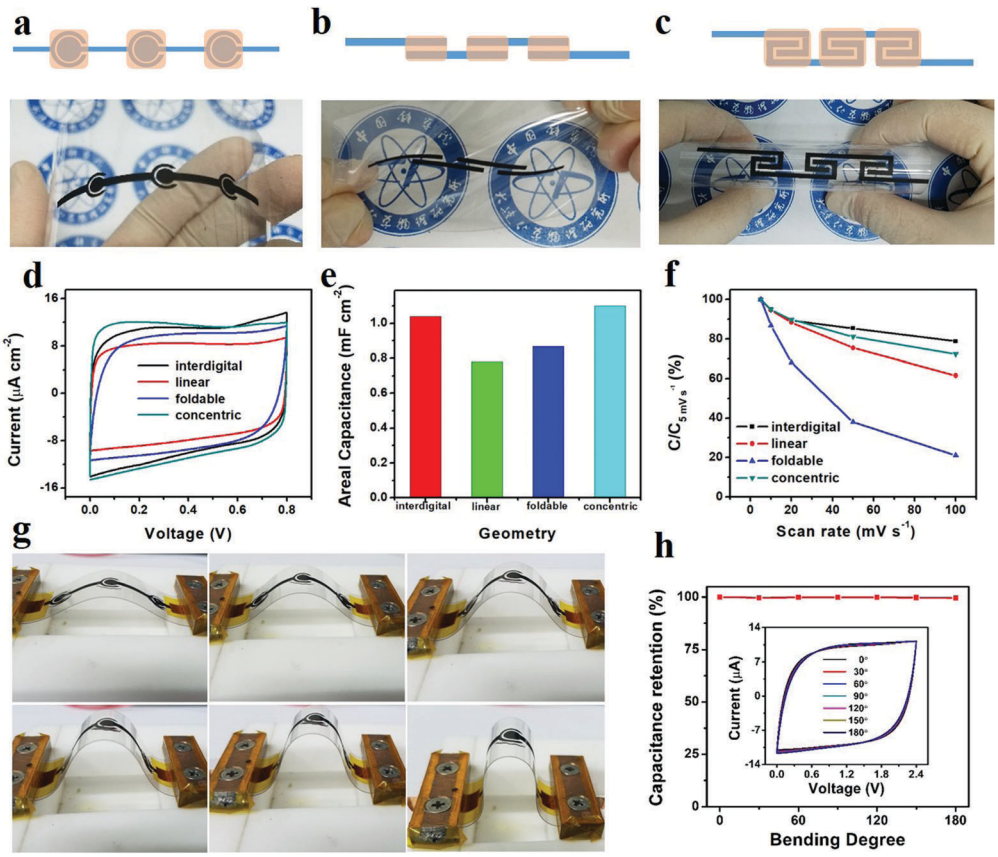

Fig. 3 Shape diversity and flexibility of tandem SPG-IMSCs. (a–c) Schematics and photographs of shape-designable SPG-IMSCs, with (a) concentric, (b) linear, and (c) foldable geometries, connecting three cells in series. Blue and yellow parts represent solidified graphene ink and PVA/H_3PO_4 electrolyte, respectively, in which the covered graphene patterns by the electrolyte are microelectrodes and the uncovered patterns are interconnects. (d) CV curves and (e) areal capacitances of SPG-MSCs with different geometries obtained at a scan rate of 5 mV s^{-1}. (f) Capacitance retention of SPG-MSCs with different geometries at diverse scan rates compared to their capacitance at 5 mV s^{-1}. (g) Photographs of SPG-IMSCs with three concentric-shaped SPG-MSCs, tested in different bending states. (h) Capacitance retention of SPG-IMSCs obtained in different bending states compared to that in the flat state. Inset: CV curves measured at 100 mV s^{-1}.

and excellent performance uniformity, supported by their CV and GCD tests (Fig. S15–S17, ESI‡). To demonstrate the outstanding mechanical flexibility of the shape-designable devices, we examined the CV curves of concentric- and strip-shaped SPG-IMSCs in different bending states (Fig. 3g and Fig. S18, ESI‡). Notably, all the CV curves remained almost coincident and only showed negligible capacitance fluctuation, *e.g.*, less than 0.5%, observed at a high bending angle of 180° (Fig. 3h). Such outstanding flexibility is mainly attributed to the elaborate design and full considerations of the planar geometry and 2D unique structure of high-quality graphene, remarkable integrity of microelectrodes and interconnects, and use of gel electrolyte, imparting enormous potential to seamless integration of SPG-IMSCs with flexible microelectronics.

Integration and ultrahigh output voltages

To satisfy the demands of future microelectronics, developing integrated power sources with tailored voltage and capacitance output is highly required. Because of the outstanding electrical conductivity, rheological properties, and electrochemical performance of graphene ink for MSCs, it is anticipated that such stable and conductive graphene ink can simultaneously act as microelectrodes and interconnects for scalable production of IMSCs, with highly adjustable voltage and capacitance output according to actual requirements. To demonstrate this feature, we fabricated a series of complex modular SPG-IMSCs (xS × yP), in which x and y represent the number of cells connected in series and in parallel, respectively. Using this printing technique, integrated devices composed of hundreds of cells are capable of instantaneous modularization within seconds (Video 1, ESI‡), showing enormous potential in the industrialization of SPG-IMSCs. Fig. 4a and b show a typical demonstration of flexible SPG-IMSCs (10S × 5P) made of 50 cells, arranged as five in parallel rows of ten serially-connected cells on a PET substrate. As expected, all the CV curves of SPG-IMSCs (xS × 1P, x = 1–10) connected in an in-series fashion from 1 to 10 cells, obtained at 100 mV s^{-1}, exhibited nearly rectangular shapes with typical EDLC behaviours (Fig. 4c), and accordingly a stepwise linear increase in the working voltage from 0.8 to 8.0 V, while the current and capacitance monotonically decreased (Fig. 4c and d).

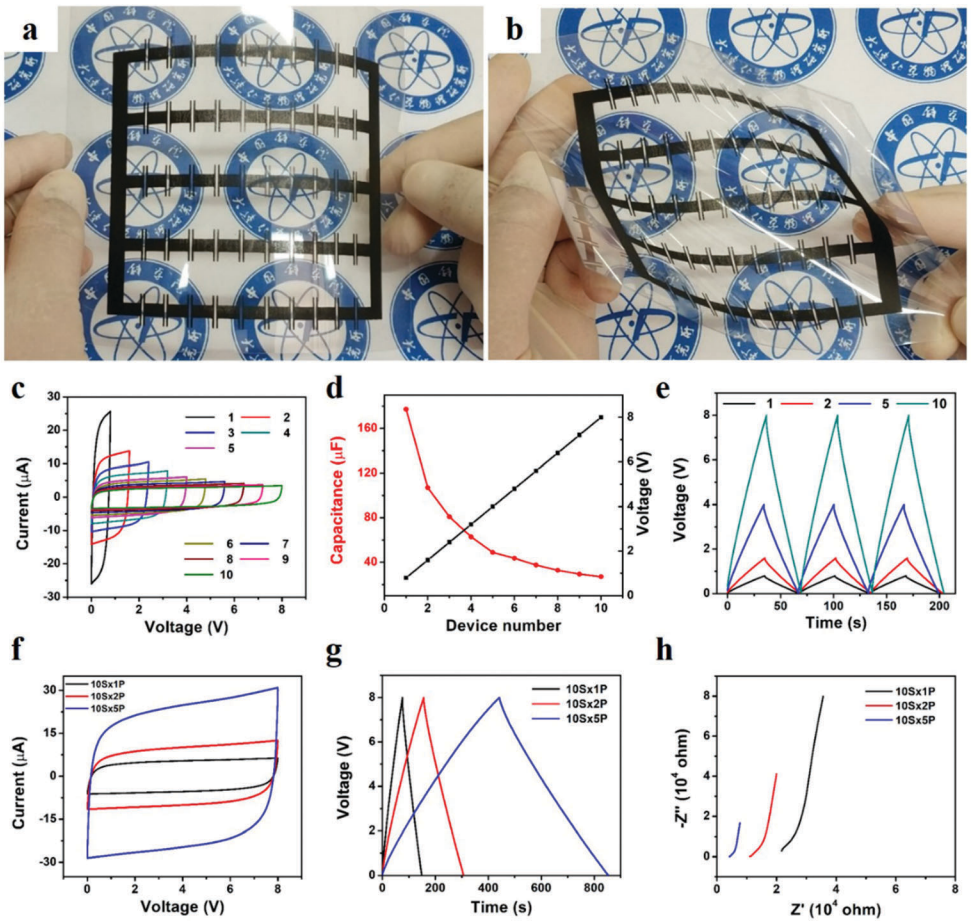

Fig. 4 Superior performance uniformity of SPG-IMSCs connected in a 10S × 5P fashion. Photographs of SPG-IMSCs(10S × 5P) in (a) flat and (b) twisted states. (c) CV curves of SPG-IMSCs connected in a tandem fashion of 1S × 1P, 2S × 1P, …, 10S × 1P, obtained at 100 mV s^{-1}. (d) Output voltage and capacitance as functions of serial cell number, calculated from Fig. 4c. (e) GCD profiles of SPG-IMSCs connected in a serial fashion of 1S × 1P, 2S × 1P, 5S × 1P, and 10S × 1P, measured at 6 μA. (f) CV curves obtained at 200 mV s^{-1}, (g) GCD profiles tested at 3 μA, and (h) the complex plane plot of SPG-IMSCs connected in serial and parallel fashions of 10S × 1P, 10S × 2P, and 10S × 5P.

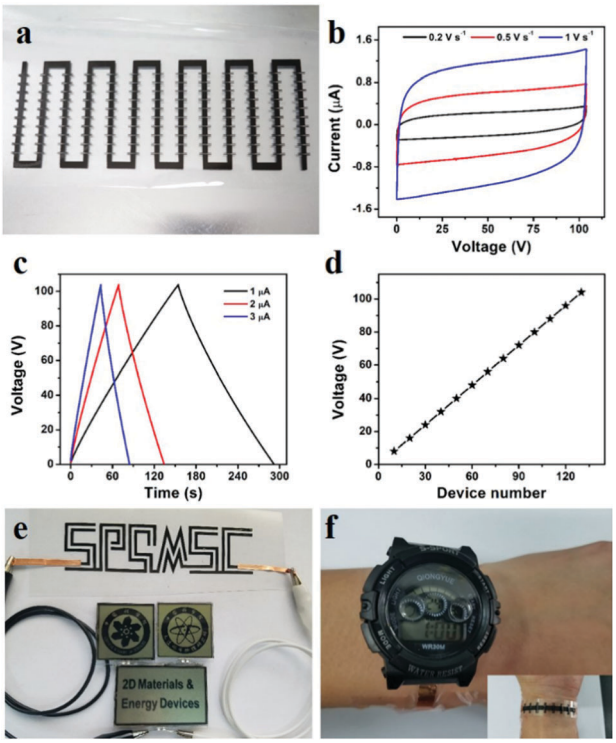

Fig. 5 Ultrahigh voltage output and aesthetic versatility of SPG-IMSCs. (a) Photograph of a tandem energy storage pack of SPG-IMSCs consisting of 130 serially-connected cells. (b) CV curves of the 104 V SPG-IMSC measured at scan rates of 0.2, 0.5, and 1 V s^{-1}. (c) GCD profiles of the 104 V SPG-IMSC obtained at varying currents of 1, 2, and 3 μA. (d) Output voltage of SPG-IMSCs as a function of serial cell number. (e) Demonstration of a letter-shaped SPG-IMSC pack for powering 3 LCDs. (f) Demonstration of powering a sports watch with a SPG-IMSC pack connecting 8 cells in series. Inset: Photograph of the integrated system of an SPG-IMSC with a sports watch.

Such remarkable tandem capacitive behaviours were also validated by GCD profiles (Fig. 4e), with symmetrical triangle shapes and invariable charge/discharge time, indicative of outstanding performance uniformity (Fig. S20, ESI‡). More importantly, the overall capacitance output can readily be enhanced using an in-parallel cell pack of SPG-IMSCs (10S × yP, y = 1–5). As shown in Fig. 4f and g, SPG-IMSCs (10S × 2P) and SPG-IMSCs (10S × 5P) delivered nearly double and quintuple capacitance in comparison with SPG-IMSCs (10S × 1P), while the operational voltage (8.0 V) remained unchanged. The ideal tandem and parallel capacitive behaviours were also well illustrated by an EIS test, in which the equivalent series resistance (ESR) was roughly inversely proportional to the increase of in-parallel rows of an in-series cell pack (Fig. 4h). Therefore, our technique is highly capable of cost-effective mass production of integrated microscale energy storage packs with tailored performance to meet the varying requirements in actual situations.

To further highlight the superior modularization of our SPG-IMSCs, ultrahigh-voltage tandem SPG-IMSCs, consisting of in-series 130 cells, were constructed (Video 2, ESI‡), as shown in Fig. 5a. As expected, a series of CV curves from the in-series 130 cells showed nearly rectangular shapes even at a high scan rate of 10 V s^{-1}, and GCD profiles displayed almost symmetrical triangles at different currents (Fig. 5b–d and Fig. S21, ESI‡), indicative of ideal EDLC behaviours. Remarkably, our modular SPG-IMSCs could stably output an ultra-high voltage of 104 V, the highest value of state-of-the-art printable supercapacitors reported to date. This is a great advancement of one-step modularization of hundreds of microscale supercapacitors, using highly-conducting and capacitive graphene ink as both microelectrodes and interconnects, which cannot be achieved by conventional supercapacitors manually connected by metal interconnects.

Besides performance engineering, the aesthetic versatility and arbitrary shapes of IMSCs for on-chip energy storage are highly required to directly integrate IMSCs into miniature electronics. To demonstrate the aesthetic versatility of SPG-IMSCs, we manufactured a letter-shaped "SPG-MSC" composed of 6 serially-connected cells, which can directly serve as stand-alone microscale power sources to light three liquid crystal displays (LCDs), showing our laboratory name "2D Materials & Energy Devices", the logo of the "Dalian Institute of Chemical Physics", and the "Chinese Academy of Sciences" (Fig. 5e). Another demonstration of our SPG-IMSCs with 8 cells connected in series could be readily integrated into a sports watch, and thus power this watch for a long time (Fig. 5f). Notably, shape-tailored SPG-IMSCs were readily printed on clothes (Fig. S22, ESI‡), revealing broad applicability.

Conclusions

In summary, we have developed a rapid, cost-effective, industrially applicable strategy for scalable production of planar IMSCs based on screen-printed graphene materials, with ultrahigh voltage output, good shape diversity, excellent aesthetic versatility, remarkable mechanical flexibility, and superior modularization on various substrates. The combination of the intriguing features of graphene and an advanced screen printing technique significantly simplifies the fabrication process and facilitates integration of planar SPG-IMSCs into printed electronics. Such a high-voltage printable energy storage pack is highly robust for powering various printed microelectronics. Most importantly, our printing technique could fabricate on-chip IMSCs with lightweight, flexibility, aesthetic properties and tailored performance in diverse substrates, indicative of its enormous potential as stand-alone miniaturized power source-utilized electronics that work in tight and small spaces in the aerospace, military, precision instrument, materials, bio-medical and other fields. Compared to the well-established photolithographic techniques, our strategy is a simple, cost-effective, highly scalable approach for fast construction of shape-tailorable IMSCs with ultrahigh voltage output and in form factors, and offers good opportunities of IMSCs for miniaturized and printed electronics.

Conflicts of interest

There are no conflicts to declare.

Acknowledgements

This work was financially supported by the National Key R&D Program of China (Grant 2016YFB0100100 and 2016YFA0200200), the National Natural Science Foundation of China (Grant 51572259, 51872283, 21805273 and 51872295), the Natural Science Foundation of Liaoning Province (Grant 201602737 and 20180510038), DICP (DICP ZZBS201708), the Dalian National Laboratory For Clean Energy (DNL), CAS, DICP&QIBEBT (Grant DICP&QIBEBT UN201702), the DNL Cooperation Fund, CAS (DNL180310, DNL180308), the Exploratory Research Program of Shaanxi Yanchang Petroleum (Group) Co. Ltd & DICP.

Notes and references

1 T. Li, G. Li, Y. Liang, T. Cheng, J. Dai, X. Yang, B. Liu, Z. Zeng, Z. Huang and Y. Luo, *Sci. Adv.*, 2017, **3**, e1602045.
2 S. Bauer, S. Bauer-Gogonea, I. Graz, M. Kaltenbrunner, C. Keplinger and R. Schwodiauer, *Adv. Mater.*, 2014, **26**, 149–162.
3 L. Hines, K. Petersen and M. Sitti, *Adv. Mater.*, 2016, **28**, 3690–3696.
4 S. Wang, J. Xu, W. Wang, G. N. Wang, R. Rastak, F. Molina-Lopez, J. W. Chung, S. Niu, V. R. Feig, J. Lopez, T. Lei, S. K. Kwon, Y. Kim, A. M. Foudeh, A. Ehrlich, A. Gasperini, Y. Yun, B. Murmann, J. B. Tok and Z. Bao, *Nature*, 2018, **555**, 83–88.
5 H. Sun, X. Fu, S. Xie, Y. Jiang and H. Peng, *Adv. Mater.*, 2016, **28**, 2070–2076.
6 X. Li, W. Cai, K. S. Teh, M. Qi, X. Zang, X. Ding, Y. Cui, Y. Xie, Y. Wu, H. Ma, Z. Zhou, Q. A. Huang, J. Ye and L. Lin, *ACS Appl. Mater. Interfaces*, 2018, **10**, 26357–26364.
7 M. F. El-Kady, V. Strong, S. Dubin and R. B. Kaner, *Science*, 2012, **335**, 1326–1330.
8 D. Pech, M. Brunet, H. Durou, P. Huang, V. Mochalin, Y. Gogotsi, P. L. Taberna and P. Simon, *Nat. Nanotechnol.*, 2010, **5**, 651–654.
9 X. Shi, Z.-S. Wu, J. Qin, S. Zheng, S. Wang, F. Zhou, C. Sun and X. Bao, *Adv. Mater.*, 2017, **29**, 1703034.
10 S. Zheng, X. Tang, Z.-S. Wu, Y. Z. Tan, S. Wang, C. Sun, H.-M. Cheng and X. Bao, *ACS Nano*, 2017, **11**, 2171–2179.
11 N. A. Kyeremateng, T. Brousse and D. Pech, *Nat. Nanotechnol.*, 2017, **12**, 7–15.
12 K.-H. Choi, D. B. Ahn and S.-Y. Lee, *ACS Energy Lett.*, 2018, **3**, 220–236.
13 Z. Niu, L. Liu, L. Zhang, W. Zhou, X. Chen and S. Xie, *Adv. Energy Mater.*, 2015, **5**, 1500677.
14 Z.-S. Wu, Y. Sun, Y.-Z. Tan, S. Yang, X. Feng and K. Müllen, *J. Am. Chem. Soc.*, 2012, **134**, 19532–19535.
15 S. Zheng, Z.-S. Wu, S. Wang, H. Xiao, F. Zhou, C. Sun, X. Bao and H.-M. Cheng, *Energy Storage Mater.*, 2017, **6**, 70–97.
16 L. Liu, Z. Niu and J. Chen, *Chem. Soc. Rev.*, 2016, **45**, 4340–4363.
17 J. Zhao, H. Li, C. Li, Q. Zhang, J. Sun, X. Wang, J. Guo, L. Xie, J. Xie, B. He, Z. Zhou, C. Lu, W. Lu, G. Zhu and Y. Yao, *Nano Energy*, 2018, **45**, 420–431.
18 J. Zhao, L. Li, Y. Zhang, C. Li, Q. Zhang, J. Peng, X. Zhao, Q. Li, X. Wang, J. Xie, J. Sun, B. He, C. Lu, W. Lu, T. Zhang and Y. Yao, *Energy Storage Mater.*, 2018, **15**, 315–323.
19 Z.-S. Wu, W. Ren, D.-W. Wang, F. Li, B. Liu and H.-M. Cheng, *ACS Nano*, 2010, **4**, 5835–5842.
20 Q. Zhang, X. Wang, Z. Pan, J. Sun, J. Zhao, J. Zhang, C. Zhang, L. Tang, J. Luo, B. Song, Z. Zhang, W. Lu, Q. Li, Y. Zhang and Y. Yao, *Nano Lett.*, 2017, **17**, 2719–2726.
21 Q. Zhang, W. Xu, J. Sun, Z. Pan, J. Zhao, X. Wang, J. Zhang, P. Man, J. Guo, Z. Zhou, B. He, Z. Zhang, Q. Li, Y. Zhang, L. Xu and Y. Yao, *Nano Lett.*, 2017, **17**, 7552–7560.
22 Z. Zhou, Q. Zhang, J. Sun, B. He, J. Guo, Q. Li, C. Li, L. Xie and Y. Yao, *ACS Nano*, 2018, **12**, 9333–9341.
23 S. Liu, P. Gordiichuk, Z.-S. Wu, Z. Liu, W. Wei, M. Wagner, N. Mohamed-Noriega, D. Wu, Y. Mai, A. Herrmann, K. Müllen and X. Feng, *Nat. Commun.*, 2015, **6**, 8817.
24 M. Zhang, Q. Zhou, J. Chen, X. Yu, L. Huang, Y. Li, C. Li and G. Shi, *Energy Environ. Sci.*, 2016, **9**, 2005–2010.
25 J. Chmiola, C. Largeot, P.-L. Taberna, P. Simon and Y. Gogotsi, *Science*, 2010, **328**, 480–483.
26 M. Zhang, X. Yu, H. Ma, W. Du, L. Qu, C. Li and G. Shi, *Energy Environ. Sci.*, 2018, **11**, 559–565.
27 F. Zhou, H. Huang, C. Xiao, S. Zheng, X. Shi, J. Qin, Q. Fu, X. Bao, X. Feng, K. Müllen and Z.-S. Wu, *J. Am. Chem. Soc.*, 2018, **140**, 8198–8205.
28 X. Peng, L. Peng, C. Wu and Y. Xie, *Chem. Soc. Rev.*, 2014, **43**, 3303–3323.
29 Y. Xia, T. S. Mathis, M.-Q. Zhao, B. Anasori, A. Dang, Z. Zhou, H. Cho, Y. Gogotsi and S. Yang, *Nature*, 2018, **557**, 409–412.
30 M. R. Lukatskaya, S. Kota, Z. Lin, M.-Q. Zhao, N. Shpigel, M. D. Levi, J. Halim, P.-L. Taberna, M. W. Barsoum, P. Simon and Y. Gogotsi, *Nat. Energy*, 2017, **2**, 17105.
31 H. Xiao, Z.-S. Wu, L. Chen, F. Zhou, S. Zheng, W. Ren, H.-M. Cheng and X. Bao, *ACS Nano*, 2017, **11**, 7284–7292.
32 Z.-S. Wu, Y. Zheng, S. Zheng, S. Wang, C. Sun, K. Parvez, T. Ikeda, X. Bao, K. Müllen and X. Feng, *Adv. Mater.*, 2017, **29**, 1602960.
33 Y. Wang, W. Lai, N. Wang, Z. Jiang, X. Wang, P. Zou, Z. Lin, H. J. Fan, F. Kang, C.-P. Wong and C. Yang, *Energy Environ. Sci.*, 2017, **10**, 941–949.
34 H. Zhang, *ACS Nano*, 2015, **9**, 9451–9469.
35 T. M. Dinh, K. Armstrong, D. Guay and D. Pech, *J. Mater. Chem. A*, 2014, **2**, 7170–7174.
36 M. F. El-Kady and R. B. Kaner, *Nat. Commun.*, 2013, **4**, 1475.
37 J. Lin, Z. Peng, Y. Liu, F. Ruiz-Zepeda, R. Ye, E. L. Samuel, M. J. Yacaman, B. I. Yakobson and J. M. Tour, *Nat. Commun.*, 2014, **5**, 5714.
38 S. Wang, Z.-S. Wu, S. Zheng, F. Zhou, C. Sun, H.-M. Cheng and X. Bao, *ACS Nano*, 2017, **11**, 4283–4291.
39 K.-H. Choi, J. Yoo, C. K. Lee and S.-Y. Lee, *Energy Environ. Sci.*, 2016, **9**, 2812–2821.
40 J. Li, S. S. Delekta, P. Zhang, S. Yang, M. R. Lohe, X. Zhuang, X. Feng and M. Östling, *ACS Nano*, 2017, **11**, 8249–8256.
41 Z. Liu, Z.-S. Wu, S. Yang, R. Dong, X. Feng and K. Müllen, *Adv. Mater.*, 2016, **28**, 2217–2222.

42 Z.-S. Wu, Z. Liu, K. Parvez, X. Feng and K. Müllen, *Adv. Mater.*, 2015, **27**, 3669–3675.
43 S. Liu, J. Xie, H. Li, Y. Wang, H. Y. Yang, T. Zhu, S. Zhang, G. Cao and X. Zhao, *J. Mater. Chem. A*, 2014, **2**, 18125–18131.
44 Y. Xu, M. G. Schwab, A. J. Strudwick, I. Hennig, X. Feng, Z. Wu and K. Müllen, *Adv. Energy Mater.*, 2013, **3**, 1035–1040.
45 Y. Jiang, Z. Xu, T. Huang, Y. Liu, F. Guo, J. Xi, W. Gao and C. Gao, *Adv. Funct. Mater.*, 2018, **28**, 1707024.
46 C. Zhu, T. Liu, F. Qian, T. Y. Han, E. B. Duoss, J. D. Kuntz, C. M. Spadaccini, M. A. Worsley and Y. Li, *Nano Lett.*, 2016, **16**, 3448–3456.
47 J. Zhao, Y. Zhang, Y. Huang, J. Xie, X. Zhao, C. Li, J. Qu, Q. Zhang, J. Sun, B. He, Q. Li, C. Lu, X. Xu, W. Lu, L. Li and Y. Yao, *Adv. Sci.*, 2018, **5**, 1801114.
48 Y. Lin, Y. Gao, F. Fang and Z. Fan, *Nano Res.*, 2018, **11**, 3065–3087.
49 Z.-S. Wu, K. Parvez, X. Feng and K. Müllen, *Nat. Commun.*, 2013, **4**, 2487.
50 W. Gao, N. Singh, L. Song, Z. Liu, A. L. Reddy, L. Ci, R. Vajtai, Q. Zhang, B. Wei and P. M. Ajayan, *Nat. Nanotechnol.*, 2011, **6**, 496–500.
51 Z.-S. Wu, K. Parvez, X. Feng and K. Müllen, *J. Mater. Chem. A*, 2014, **2**, 8288–8293.

